Coupling of N_2O decomposition and ethylbenzene dehydrogenation over γ-Al_2O_3-supported transition metal oxide catalysts

Piotr Kuśtrowski [a,*], Małgorzata Zbroja [a], Roman Dziembaj [a], and Helmut Papp [b]

[a] *Faculty of Chemistry, Jagiellonian University, Ingardena 3, 30-060 Kraków, Poland*
[b] *Institut für Technische Chemie, University of Leipzig, Linnéstrasse 3, 04103 Leipzig, Germany*

Received 18 September 2001; accepted 14 January 2002

Transition metal (Cr, Cu, Fe, Co and Ni) oxides supported on γ-alumina were characterized with respect to their textural parameters and reducibility and used as catalysts in decomposition of nitrous oxide and ethylbenzene (EB) dehydrogenation as well as coupling of both processes. High activity of γ-Al_2O_3 in N_2O decomposition coupled with EB dehydrogenation has been found. An increase in EB and N_2O conversion was observed when transition-metal-containing catalysts were used. The activity of catalysts depended on their reducibility. Maximum N_2O efficiency was observed for the Cr/γ-Al_2O_3 sample, whereas γ-Al_2O_3-supported Cu and Fe oxide systems showed about 50% efficiency of N_2O in the reaction. An influence of the molar ratio of N_2O/EB on activity and selectivity of the catalysts was found. An excess of N_2O resulted in an increase in CO_2 formation at nearly constant styrene yield.

KEY WORDS: nitrous oxide decomposition; oxidative dehydrogenation; ethylbenzene; transition metal oxides; supported catalysts; TPR; BET.

1. Introduction

N_2O is a by-product in industrial plants from the production of adipic and nitric acid, and from the combustion of fossil fuels and biomass. It is also formed from land cultivation, the regeneration of coked fluid cracking catalysts and the non-selective catalytic reduction of NO_x with ammonia [1]. These sources of N_2O emission cause its concentration to increase in the atmosphere at a rate of about 0.3% per year. The concentration has now reached *ca.* 310 ppb [2]. Despite this seemingly low concentration, nitrous oxide is strongly involved in the atmospheric greenhouse effect because each molecule of N_2O present in the atmosphere is characterized by an average lifetime of about 150 years and a net greenhouse effect of about 300 times greater than that of CO_2 [3].

The emission of N_2O can be reduced by improvement of currently used technology (*e.g.* application of more selective catalysts for the above-mentioned processes), or by catalytic decomposition of N_2O into nitrogen and oxygen, as well as use of nitrous oxide as a mild oxidizing agent in selective oxidation (or dehydrogenation) of hydrocarbons. Thus, Suzuki *et al.* [4] described the performance of N_2O in direct hydroxylation of benzene to phenol on H-ZSM-5. This was the basis for further research leading to iron complexes stabilized in a ZSM-5 matrix generating surface α-oxygen species from nitrous oxide [5] and to the application of ZSM-5 type zeolites as active, selective and stable catalysts in selective oxidation of aromatic compounds (alkyl-, chloro- and fluorobenzenes as well as phenol) into corresponding phenols and diphenols [6]. N_2O was used further as a mild oxidant, *e.g.* in partial oxidation of ethane to ethylene and acetaldehyde over supported molybdenum [7] and vanadium [8] catalysts, and in oxidative dehydrogenation of *n*-butane on MgO-supported vanadium oxide catalysts [9].

Oxidative dehydrogenation of ethylbenzene (EB) is the most attractive alternative method for the production of styrene due to thermodynamic and energetic reasons [10–12]. Use of oxidant results in achievement of higher degree of EB conversion at significantly lower temperatures than in the classical process of styrene production. The strong reactivity of oxygen causes, however, burning of considerable amounts of ethylbenzene to CO_x. SO_2 [13] and CO_2 [14,15] were proposed as milder oxidizing agents. Using sulphur dioxide at an industrial scale is, however, impossible because many toxic and corrosive by-products (*e.g.* benzothiophene, CS_2, COS) are formed in the process. In spite of this, the application of CO_2 is very effective, fast deactivation of the catalysts being observed due to the formation of inactive carbonaceous deposits [16].

Following up promising results of López Nieto *et al.* [9] and seeking to find an effective oxidant agent for dehydrogenation of ethylbenzene, we have proposed the utilization of N_2O in the above-mentioned process. This work presents results of catalytic tests performed on a series of transition metal oxides supported on γ-alumina in the decomposition of nitrous oxide and EB dehydrogenation, as well as coupling of both reactions.

* To whom correspondence should be addressed.

1011-372X/02/0500-0001/0

2. Experimental

γ-Al_2O_3 (Merck) was used as a support. Catalysts were prepared by an incipient wetness technique with aqueous solutions of $Cr(NO_3)_3 \cdot 9H_2O$, $Cu(NO_3)_2 \cdot 3H_2O$, $Co(NO_3)_2 \cdot 6H_2O$, $Fe(NO_3)_3 \cdot 9H_2O$ or $Ni(NO_3)_2 \cdot 6H_2O$. The amount of salts was adjusted to obtain the transition metal contents given in table 1. The precursors were dried at 180 °C for 2 h and then calcined in air at 600 °C for 3 h.

Textural parameters of the catalysts were determined by N_2 sorption at 77 K using an ASAP 2010 (Micromeritics) after outgassing the samples at 350 °C under vacuum. The temperature-programmed reduction (TPR) of the samples containing transition metal oxides was carried out in the temperature range 100–1000 °C in a fixed bed continuous flow quartz microreactor (i.d., 5.0 mm; length, 150 mm). The H_2 consumption was monitored on-line by a thermal conductivity detector (Varian) connected to the reactor outlet by a heated line. Before TPR experiments the samples (50 mg) were outgassed in a flow of nitrogen (30 ml/min) at 120 °C for 30 min. TPR was carried out with a linear heating rate ($\beta = 20$ °C/min) in a flow of reducing mixture of 5.22% H_2 in Ar (15 ml/min).

Catalytic tests were performed in a plug flow microreactor (i.d., 4.5 mm; length, 240 mm). 100 mg of the catalyst was loaded at the central position of the reactor onto a quartz wool plug. The flow of gaseous reactants (5 vol% N_2O in He) was controlled by mass flow controllers (Brooks 5850E). Ethylbenzene was fed to the reaction system with a syringe pump (Cole-Parmer 74900). The reaction products were monitored by a gas chromatograph (Varian CP-3800) equipped with three capillary columns—CP-8 (for separation of aromatic compounds), Poraplot Q (for CO_2, H_2O, N_2O), Molsieve 5A (for N_2, O_2, CO)—and two detectors—TCD and mass spectrometer Saturn 2000 (Varian). The sample of reactants was collected directly from the outlet of the reactor using a six-port valve (Valco).

The catalytic activity was studied for N_2O decomposition as well as EB dehydrogenation in helium or in the presence of N_2O. Prior to the decomposition of N_2O the catalysts were activated at 350 °C for 40 min in the flow of N_2O (0.4 ml/min) diluted with He (up to a total flow of 50.0 ml/min). The pretreatment procedure for EB dehydrogenation depended on the molar ratio of N_2O/EB used during the reaction, *i.e.* the catalysts were pretreated in a mixture of N_2O (0, 0.4 or 0.8 ml/min) in He (up to a total flow of 49.6 ml/min) at 350 °C for 40 min. Then dosing of EB (130 μl liquid EB/h $\approx$ 0.40 ml EB vapour/min) began. The first GC analysis (regardless of the type of reaction) was performed after 10 min. The temperature of the catalyst bed was increased from 350 °C to 550 °C in 50 °C steps with three analyses of products (at 20 min intervals) at each step.

Table 1
Composition and textural properties of γ-Al_2O_3-supported catalysts

Sample	Transition metal content (wt%)	BET surface area (m^2/g)	Total pore volume (cm^3/g)	Average pore diameter (Å)
γ-Al_2O_3	–	193 (220) [a]	0.49 (0.50) [a]	101 (91) [a]
Co/γ-Al_2O_3	8.4	170	0.41	96
Cu/γ-Al_2O_3	9.2	173	0.43	100
Cr/γ-Al_2O_3	7.5	192	0.42	87
Fe/γ-Al_2O_3	7.7	176	0.42	95
Ni/γ-Al_2O_3	8.4	178	0.44	98

[a] Values in parentheses refer to the non-calcined support.

3. Results and discussion

3.1. Catalyst characterization

All N_2 adsorption isotherms were of type IV, showing a mesoporous character of the solids. Moreover, the hysteresis in the desorption branch (type H1 according to [17]) allows cylindrical pores of uniform size to be assumed. The calcination of the support caused a only slight decrease of the specific surface area (about 12%) and the porosity (about 3%). The results are collected in table 1. The introduction of transition metal oxides contributes to a further drop in the BET surface area (0.5–12%) and the total pore volume (10–16%). The average pore size calculated using the BJH method varied from 87 to 100 Å for all the catalysts. This means that the impregnation followed by thermal decomposition has not caused blocking of the pores. This is a favourable point for catalytic and adsorptive properties since no diffusional limitations are present.

The TPR profiles of the γ-alumina-supported catalysts (figure 1) allow a preliminary characterization of the transition metal oxides on/in the support matrix. In case of the Cr/γ-Al_2O_3 sample there is a single reduction peak centred at 380 °C. On the basis of the reduction temperature and the amount of hydrogen consumed ($Cr/H_2 = 1.01$) it can be assumed that the reduction of Cr^{6+} to Cr^{3+} occurred [18], *i.e.* a formation of surface chromates, anchored onto an alumina support, from the Cr^{3+}-containing precursor took place upon calcination of the sample in air.

The TPR profile of Cu/γ-Al_2O_3 is characterized by two unresolved peaks centred at 285 and 320 °C. The amount of hydrogen consumed ($Cu/H_2 = 1.02$) is sufficient for a complete reduction of Cu^{2+} to Cu^0. The observed two-step reduction suggests the presence of various types of Cu^{2+}-containing species formed on/in the defective spinel-type structure of γ-Al_2O_3 [19]. Nevertheless, it cannot be excluded that the shape of the TPR curve originates from the applied experimental conditions [20].

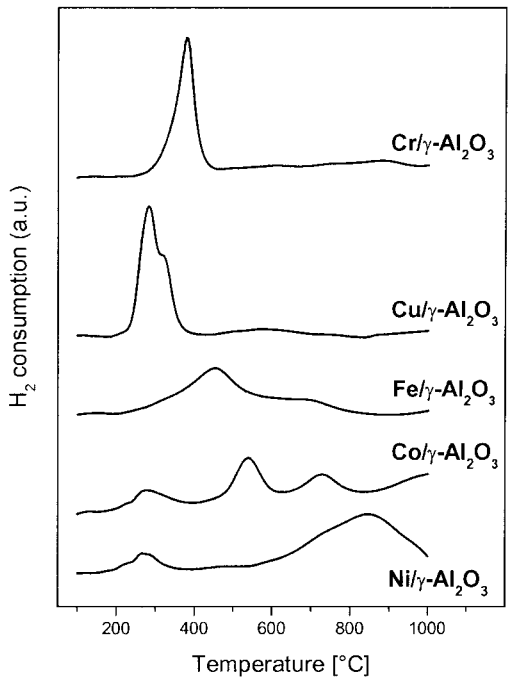

Figure 1. TPR profiles of transition metal oxides supported on γ-Al_2O_3.

In the case of Ni/γ-Al_2O_3 two reduction peaks were observed. The lower temperature peak centred at 270 °C is attributed to the reduction of Ni^{2+} in the NiO surface species to Ni^0 and the higher temperature peak at 845 °C to the reduction of Ni^{2+} to Ni^0 in $NiAl_2O_4$ formed during the calcination of the sample. The molar ratio between surface NiO and bulk $NiAl_2O_4$ was equal to 0.11 according to the amounts of hydrogen consumed within each of the reduction steps.

The reduction of Co/γ-Al_2O_3 began below 200 °C and showed maxima at 280, 540 and 730 °C. According to Arnoldy and Moulijn [21], these reduction regions can be assigned to different Co phases. The reduction of Co_3O_4 crystallites took place in the lowest temperature range of 160–400 °C. In the next step (400–630 °C) surface Co^{3+} ions and/or mixed Co–Al–oxide, where Co^{3+} ions occupy the octahedral sites and Al^{3+} are localized in the tetrahedral sites, were reduced. Reduction in the temperature region of 630–830 °C corresponds to surface Co^{2+} ions. Above 830 °C the reduction of the $CoAl_2O_4$ phase began.

Iron(III) oxide supported on γ-Al_2O_3 showed the TPR profile typical for a haematite phase [22]. It seems as if the reduction of Fe/γ-Al_2O_3 occurs in three steps:

$$Fe_2O_3 \rightarrow Fe_3O_4 \rightarrow FeO \rightarrow Fe.$$

The maximum at 450 °C corresponds with the magnetite formation, whereas the peak centred at about 660 °C is attributed to the reduction of Fe_3O_4 to FeO. The reduction into metallic iron began above 920 °C.

3.2. Catalytic activity

It was shown in preliminary tests that N_2O decomposition and EB dehydrogenation were negligible in the absence of any catalyst within the temperature range 350–550 °C. The activities of the γ-Al_2O_3 support alone are shown in figure 2(A). The conversion of N_2O in the absence of EB did not exceed 9% at 550 °C. The dehydrogenation of EB in pure helium occurred with even lower efficiency—below 3%. But, the coupling of N_2O decomposition with the EB dehydrogenation

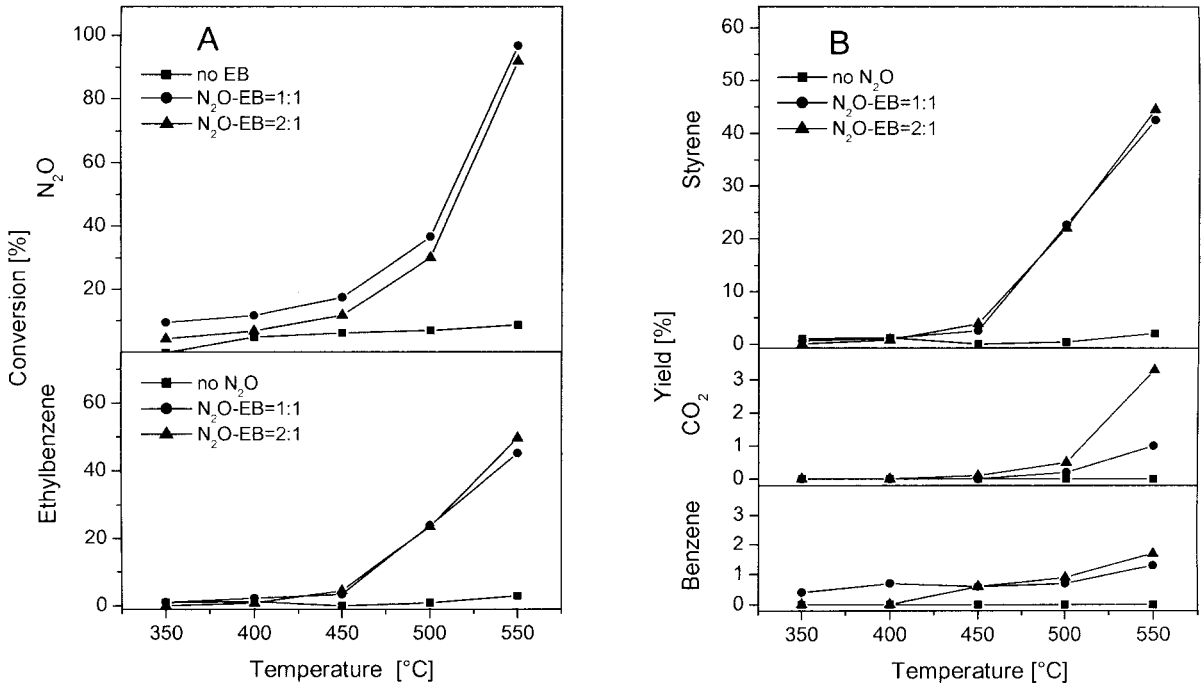

Figure 2. N_2O and EB conversions (A) and yields of carbon-containing products (B) *versus* reaction temperature on γ-Al_2O_3 at various feed compositions.

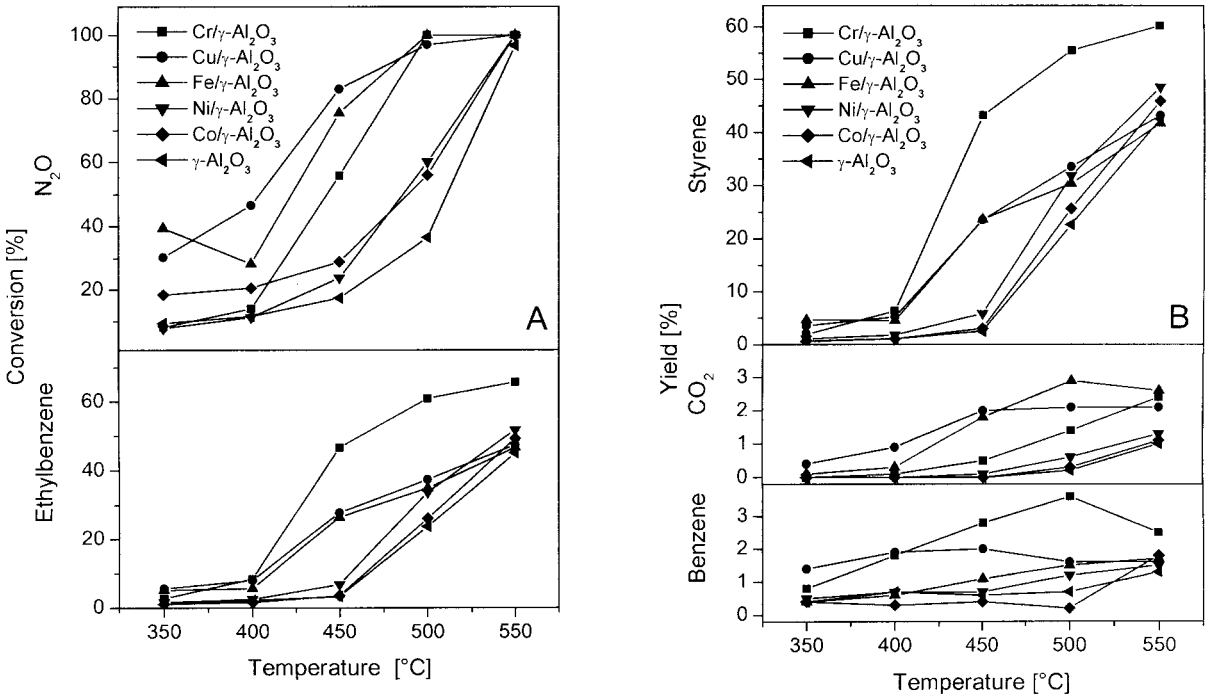

Figure 3. N_2O and EB conversions (A) and yields of carbon-containing products (B) *versus* reaction temperature on transition metal oxides supported on γ-Al_2O_3 at a molar ratio of $N_2O/EB = 1:1$.

process resulted in a significant increase in conversion of both reactions. Moreover, the selectivity of EB dehydrogenation towards styrene is nearly 90%. The yields of the main carbon-containing products (styrene, benzene and CO_2) as a function of reaction temperature are presented in figure 2(B). At a molar ratio of $N_2O/EB = 1:1$ and at the highest reaction temperature (550 °C), a yield of styrene of 42.5% was obtained, whereas the yields of benzene and CO_2 were 1.3% and 1.0% respectively. An excess of N_2O caused, however, a slight increase of the total oxidation of EB to CO_2. The great majority of the process then proceeds according to the following equation:

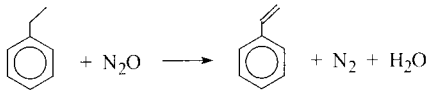

Rapid acceleration of the reaction between the adsorbed N_2O and $C_6H_5C_2H_5$ molecules, or rather their fragments, was then observed when the alumina catalyst was used. Active oxygen species generated from nitrous oxide can be responsible for this effect. However, the type of sites which catalyse the reaction is not recognized. X-ray fluorescence analysis showed that the γ-Al_2O_3 sample consists of only traces of the impurity elements: S (0.10 wt%), Ga (0.07 wt%), Fe, Cu and Zn (<0.01 wt%). Thus, high activity of alumina should not necessarily be attributed to the presence of metallic active sites. It is most likely that the reaction is catalysed by active coke formed on the catalyst surface. The redox-type mechanism of oxidative dehydrogenation of EB over acidic catalysts (like bare carbons, alumina, zeolites or phosphates), where quinoid groups from carbonaceous deposits act as the real active centres, was previously proposed for the reaction performed in the presence of oxygen [10,11,23] and supported by a series of spectroscopic studies, *e.g.* XPS, SIMS and EPR [24–29]. According to this concept, an oxidant reoxidizes reduced quinoid groups, with formation of H_2O observed among the reaction products.

A further increase in the activity of the catalysts was obtained by the presence of transition metal oxides. The results obtained with a stoichiometric mixture of EB and N_2O are presented in figure 3. The highest activity in N_2O decomposition showed Cu, Fe and Cr oxide-containing catalysts. In the case of EB dehydrogenation the catalyst series could be divided into three groups: the most active was Cr/γ-Al_2O_3 (43% of styrene yield at 450 °C), less active were Cu/γ-Al_2O_3 (24%) and Fe/γ-Al_2O_3 (23%), and the worst were Ni/γ-Al_2O_3 (6%) and Co/γ-Al_2O_3 (3%). It is especially noteworthy that there is a relationship between the observed activity in N_2O decomposition coupled with EB dehydrogenation and the TPR profiles of the catalysts. The catalysts which did not form a $Me^{II}Al_2O_4$ phase and were more easily reducible were more active in the reaction.

The effect of the molar ratio of N_2O/EB on the conversion of both reactants on three of the most active catalysts is shown in figure 4. The disappearance of N_2O was obviously much faster when the process occurred in the presence of ethylbenzene. The highest N_2O conversion was observed for the reaction at the molar ratio of

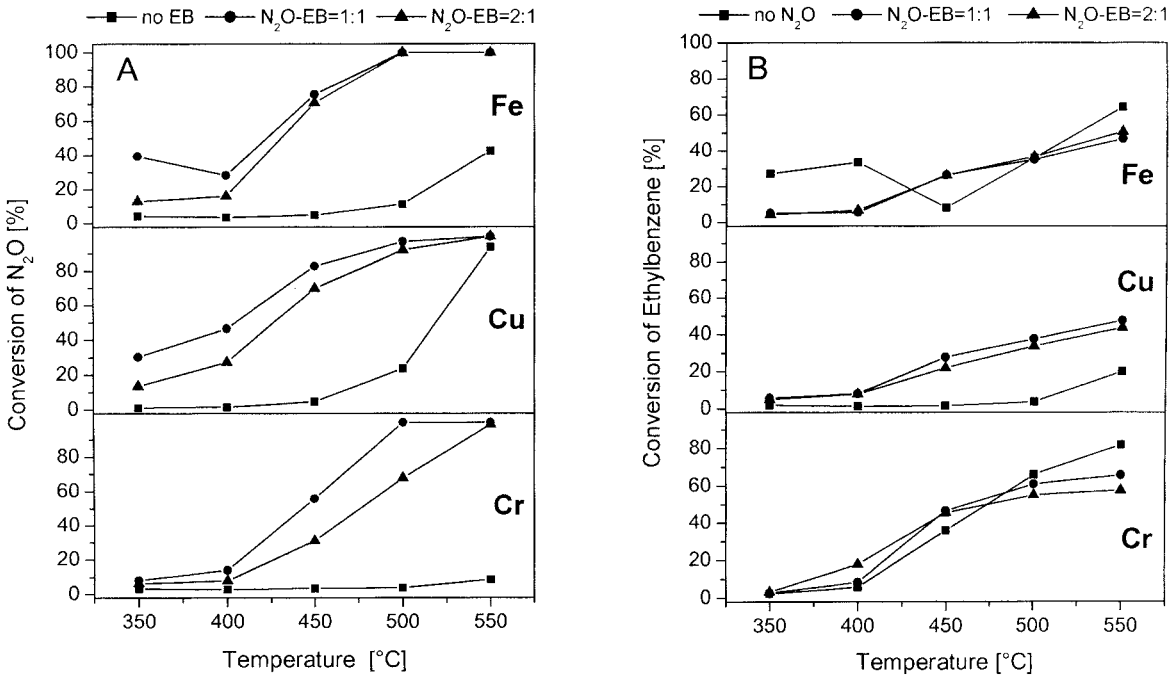

Figure 4. Conversion of N_2O (A) and EB (B) observed on three of the most active catalysts *versus* reaction temperature at various feed compositions.

$N_2O/EB = 1$. An excess of nitrous oxide resulted in a drop of the conversion of N_2O. An increase in EB conversion was noticeable, especially in the low-temperature range (350–450 °C), when N_2O was introduced into the reactant feed. The EB conversion in the absence of nitrous oxide as a function of reaction temperature showed a peculiarity for the Fe/γ-Al_2O_3 catalyst. At 350–400 °C the EB conversion was quite high (27.1–33.5%), then dropped to 8.1% at 450 °C and increased again at 550 °C reaching 64.4%. This peculiarity must be related to the phase change within the iron oxide catalyst in the temperature range 400–450 °C, where it is possible that a reduction of Fe_2O_3 by EB occurred.

Figure 5 shows the yields of styrene, CO_2 and benzene as a function of reaction temperature for the EB dehydrogenation process at various molar ratios of N_2O/EB. The highest amounts of styrene were generally obtained when the reaction was performed at a molar ratio of $N_2O/EB = 1:1$. The excess of nitrous oxide favoured CO_2 formation, especially in the case of Fe/γ-Al_2O_3 and Cu/γ-Al_2O_3 catalysts, which were the most active in N_2O decomposition.

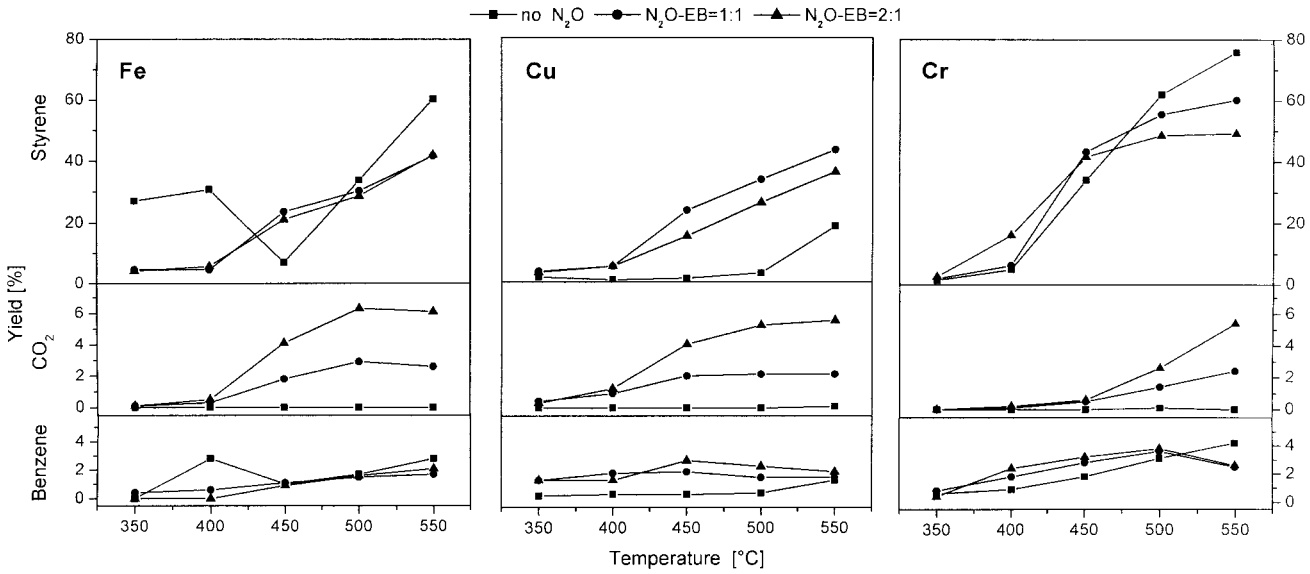

Figure 5. Yields of carbon-containing products observed on three of the most active catalysts *versus* reaction temperature at various feed compositions.

4. Conclusions

1. γ-Al_2O_3 support which was poorly active in N_2O decomposition and EB dehydrogenation showed a high catalytic performance when coupling both processes.
2. Introduction of transition metal oxides onto γ-Al_2O_3 resulted in an increase of EB and N_2O conversion. The catalysts can be ordered with respect to their activity as follows:

$$\mathrm{Cr}/\gamma\text{-}\mathrm{Al_2O_3} > \mathrm{Cu}/\gamma\text{-}\mathrm{Al_2O_3} \sim \mathrm{Fe}/\gamma\text{-}\mathrm{Al_2O_3} > \mathrm{Ni}/\gamma\text{-}\mathrm{Al_2O_3} \sim \mathrm{Co}/\gamma\text{-}\mathrm{Al_2O_3} \sim \gamma\text{-}\mathrm{Al_2O_3}.$$

   The most active catalysts are characterized by the easiest reducible surface oxide system.
3. An excess of N_2O caused an increase in total oxidation of EB to CO_2 and a drop in N_2O conversion.

References

[1] F. Kapteijn, J. Rodriguez-Mirasol and J.A. Moulijn, Appl. Catal. B 9 (1996) 25.
[2] M.A. Wojtowicz, J.R. Pels and J.A. Moulijn, Fuel Proc. Technol. 34 (1993) 1.
[3] S. Kannan, Appl. Clay Sci. 13 (1998) 347.
[4] E. Suzuki, K. Nakashiro and Y. Ono, Chem. Lett. (1988) 953.
[5] G.I. Panov, A.K. Uriarte, M.A. Rodkin and V.I. Sobolev, Catal. Today 41 (1998) 365.
[6] L.M. Kustov, A.L. Tarasov, V.I. Bogdan, A.A. Tyrlov and J.W. Fulmer, Catal. Today 61 (2000) 123.
[7] L. Mendelovici and J.H. Lunsford, J. Catal. 94 (1985) 37.
[8] A. Erdöhelyi and F. Solymosi, J. Catal. 129 (1991) 497.
[9] J.M. López Nieto, A. Dejoz, M.I. Vazquez, W. O'Leary and J. Cunningham, Catal. Today 40 (1998) 215.
[10] G. Emig and H. Hofmann, J. Catal. 84 (1983) 15.
[11] G.E. Vrieland and P.G. Menon, Appl. Catal. 77 (1991) 1.
[12] F. Cavani and F. Trifirò, Appl. Catal. A 133 (1995) 219.
[13] C.R. Adams and T.J. Jennings, J. Catal. 17 (1970) 157.
[14] M. Sugino, H. Shimada, T. Turuda, H. Miura, N. Ikenaga and T. Suzuki, Appl. Catal. A 121 (1995) 125.
[15] T. Badstube, H. Papp, P. Kuśtrowski and R. Dziembaj, Catal. Lett. 55 (1998) 169.
[16] R. Dziembaj, P. Kuśtrowski, T. Badstube and H. Papp, Top. Catal. 11/12 (2000) 317.
[17] G. Leofanti, M. Padovan, G. Tozzola and B. Venturelli, Catal. Today 41 (1998) 207.
[18] M.I. Zaki, N.E. Fouad, G.C. Bond and S.F. Tahir, Thermochim. Acta 285 (1996) 167.
[19] H. Knözinger and P. Ratnasamy, Catal. Rev.—Sci. Eng. 17 (1978) 31.
[20] G. Fierro, M. Lo Jacono, M. Inversi, P. Porta, R. Lavecchia and F. Cioci, J. Catal. 148 (1994) 709.
[21] P. Arnoldy and J.A. Moulijn, J. Catal. 93 (1985) 38.
[22] N.W. Hurst, S.J. Gentry, A. Jones and B.D. McNicol, Catal. Rev.—Sci. Eng. 24 (1982) 233.
[23] T.G. Alkhazov, A.E. Lisovskii, M.G. Safarov and A.M. Dadasheva, Kinet. Katal. 13 (1972) 509.
[24] A.E. Lisovskii and C. Aharoni, Catal. Rev.—Sci. Eng. 36 (1994) 25.
[25] R. Fiedorow, W. Przystajko, M. Sopa and I.G. Dalla Lana, J. Catal. 68 (1981) 33.
[26] A. Schraut, G. Emig and H.G. Sockel, Appl. Catal. 29 (1987) 311.
[27] A. Schraut, G. Emig and H. Hofmann, J. Catal. 112 (1988) 221.
[28] L.E. Cadus, L.A. Arrua, O.F. Gorriz and J.B. Rivarola, Ind. Eng. Chem. Res. 27 (1988) 2241.
[29] L.E. Cadus, O.F. Gorriz and J.B. Rivarola, Ind. Eng. Chem. Res. 29 (1990) 1143.